

# Single Dielectric Barrier Discharge Plasma Actuators for Improved Airfoil Performance

James H. Mabe\* and Frederick T. Calkins†  
*The Boeing Company, Seattle, Washington 98124*

and

B. Wesley,‡ R. Woszidlo,‡ L. Taubert,‡ and I. Wagnanski§  
*University of Arizona, Tucson, Arizona 85721*

DOI: 10.2514/1.37638

The applicability of single dielectric barrier discharge plasma actuators for use as active flow control devices, capable of enhancing the performance of airfoils, was assessed in this investigation. Measurements were carried out on two thick airfoils with simple flaps: a NACA0021 and an airfoil that is similar to those commonly used on tiltrotor aircraft. The chord length of the airfoils was approximately 0.3 and 0.25 m, respectively, and the span was approximately 0.6 m. They were both tested in the same wind tunnel with a test section of 0.6 × 1.1 m. Freestream velocities varying from 5 to 15 m/s were tested, corresponding to chord Reynolds numbers ranging between  $0.8 \times 10^5$  and  $3 \times 10^5$ . The lift, moment, and form drag were obtained from the pressure distributions over the airfoil's surface, and the total drag was calculated from a wake survey. The range of incidence angles  $\alpha$  varied from  $-4^\circ < \alpha < +20^\circ$  and flap deflections  $\delta_f$  of 0 and 15 deg were tested. The location of the actuation was also altered. Two data sets are presented: one in which the actuator was placed at approximately 5% of the chord and the other in which it was located just upstream of the flap shoulder at a chord location corresponding to about 75%. The momentum input of the single dielectric barrier discharge plasma actuators was measured with a hot wire and was in good agreement with previously published results. The input momentum is very weak and is not sufficient to prevent separation at Reynolds numbers greater than 100,000. The single dielectric barrier discharge plasma actuators used in this study may only provide sufficient momentum to be effective at very low Reynolds numbers, such as those appropriate to micro air vehicles. Under special circumstances, their passive presence on the surface may trip the boundary layer, making it more resistant to separation, but in those cases, a proper roughness strip or vortex generators may delay separation more effectively.

## Nomenclature

$C$	=	chord length
$C_D$	=	drag coefficient, $D/qc$
$C_L$	=	lift coefficient, $L/qc$
$C_P$	=	pressure coefficient, $(p - p_\infty)/q$
$C_\mu$	=	momentum coefficient, $(2h/c)(U_{\text{slot}}/U_\infty)^2$
$D$	=	drag
$F^+$	=	nondimensional frequency, $fx_c/U_\infty$
$f$	=	frequency of excitation
$L$	=	lift
$q$	=	dynamic pressure, $1/2\rho U_\infty^2$
$Re$	=	Reynolds number, $U_\infty c/\nu$
$t$	=	maximum thickness of the airfoil
$x_c$	=	distance from the actuator to the trailing edge
$\alpha$	=	angle of attack
$\delta_f$	=	flap deflection angle

## I. Introduction

ACTIVE flow control (AFC) improves the performance of airfoils by altering the pressure distribution over their surface (mostly over the upper loft) and being able to do so on demand. This can be achieved either in conjunction with some existing control surfaces or by replacing them altogether. AFC increases the airfoil's lifting capabilities, reduces its drag, and changes its pitching moment. It thus has the potential of replacing the complex and slow control surfaces on conventional multi-element wings. The applicability of AFC hinges on the availability of light reliable actuators that are capable of providing the necessary control authority at the required flight conditions. The single dielectric barrier discharge (SDBD) plasma actuators (PA) are attractive because they possess no moving parts, they can be easily installed anywhere on the airfoil, they consume little power, their frequency of operation is high and thus amenable to modulation or periodic interruption (the use of bursts), and they are light. Unfortunately, the momentum that they impart to the boundary layer is low, and therefore their utility may be limited.

Over the last 15 years, numerous researchers have investigated the use of plasma actuators for flow control. Single dielectric barrier discharge plasma actuators use two offset electrodes: one of which is exposed to air and the other covered by a thin dielectric material. When a high-voltage alternating potential is applied to the electrodes, the air is ionized in the region of high-voltage gradient at the edge of the exposed electrode, as shown in Fig. 1. The plasma in the area of an electric field gradient produces a body force, or net flow, near the airfoil surface [1,2]. Plasma actuators have been shown to significantly increase stall angle and reduce drag, particularly at low Reynolds numbers [3,4]; however, in laminar flow, the use of simple vortex generators may be just as effective [5,6]. Recent studies have shown that SDBD actuators that produce a higher momentum, which would be effective at high Reynolds numbers, may be possible [7]; however, the supporting technology to integrate these actuators into

Received 19 March 2008; accepted for publication 7 December 2008.  
Copyright © 2009 by The Boeing Company. Published by the American Institute of Aeronautics and Astronautics, Inc., with permission. Copies of this paper may be made for personal or internal use, on condition that the copier pay the \$10.00 per-copy fee to the Copyright Clearance Center, Inc., 222 Rosewood Drive, Danvers, MA 01923; include the code 0021-8669/09 \$10.00 in correspondence with the CCC.

\*Engineer/Scientist, Phantom Works, P.O. Box 3707, Mail Stop 42-51. Member AIAA.

†Engineer/Scientist, Aeroacoustics, P.O. Box 3707, Mail Stop 67-ML. Member AIAA.

‡Graduate Student, Aerospace and Mechanical Engineering Department. Student Member AIAA.

§Professor, Department of Aerospace and Mechanical Engineering, 1130 North Mountain Avenue. Fellow AIAA.

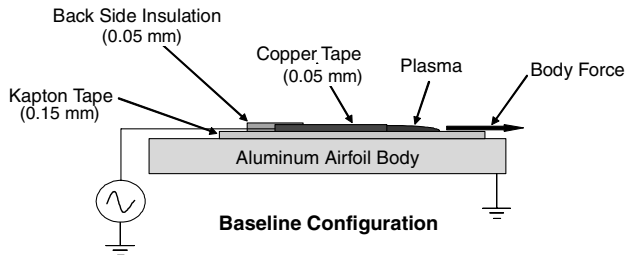


Fig. 1 Diagram of single dielectric barrier discharge plasma actuator.

an airfoil, such as specialized power amplifiers and materials capable of operating at high voltages and temperatures, requires additional maturation.

Göksel et al. [8,9] considered the effect of plasma actuation over a small airfoil (17.8 cm in chord) Eppler-338 at various low speeds corresponding to Reynolds numbers in the range of  $20,000 < Re < 140,000$ . They calibrated the output of the actuator in terms of steady and oscillatory momentum coefficients  $c_\mu$  at a number of freestream velocities. These procedures enabled them to assess the momentum imparted to the flow at each of their test conditions and to compare the performance of the plasma actuators with other more conventional devices used in AFC applications. They concluded that at  $Re = 140,000$ , the effect of the plasma actuator was actually detrimental to the lift augmentation, but as the freestream velocity was reduced and the plasma was pulsed at a duty cycle corresponding to  $F^+ = 1$ , there was a substantial increase in the lift being generated. The efficacy of the actuation increased with Reynolds number reduction, and at a Reynolds number of approximately 20,000, the maximum lift generated by the airfoil increased by about a factor of 2 at an input  $c_\mu$  of 0.05% and a duty cycle of 3%. It became obvious that at this Reynolds number, the plasma actuator prevented the massive leading-edge separation that normally occurs at low angles of incidence. This work motivated the study described in this paper.

## II. Description of the Models and the Experimental Apparatus

The 2 airfoil models tested in this study are shown in Fig. 2. Both are hollow and can internally accommodate a variety of actuators, power cables, and pressure tubing. The flaps are hollowed for the same purpose. Both have been previously tested using other forms of active flow control and were selected for this reason. Pressure taps cover the wing and flap for form drag and lift measurements in both airfoils. All pressure measurements had an accuracy and repeatability of  $\pm 1\%$ . The tiltrotor airfoil has a simple flap and also a slightly modified cove that avoids the cavity existing on the lower loft of the original airfoil that uses a Fowler action. Such a cavity not only increases the drag, but also generates noise.

Figure 3 shows the NACA0021 airfoil section in the wind tunnel in which it spans the tunnel walls with pressure taps connected to a scanner located on the roof of the test section. The airfoil is mounted on a turntable that is attached to a stepper motor, allowing it to rotate and change the angle of attack under computer control. The flap deflection angle had to be adjusted manually from outside the tunnel. A rake of pitot tubes located approximately two chord lengths downstream of the airfoil measured its drag by assessing the

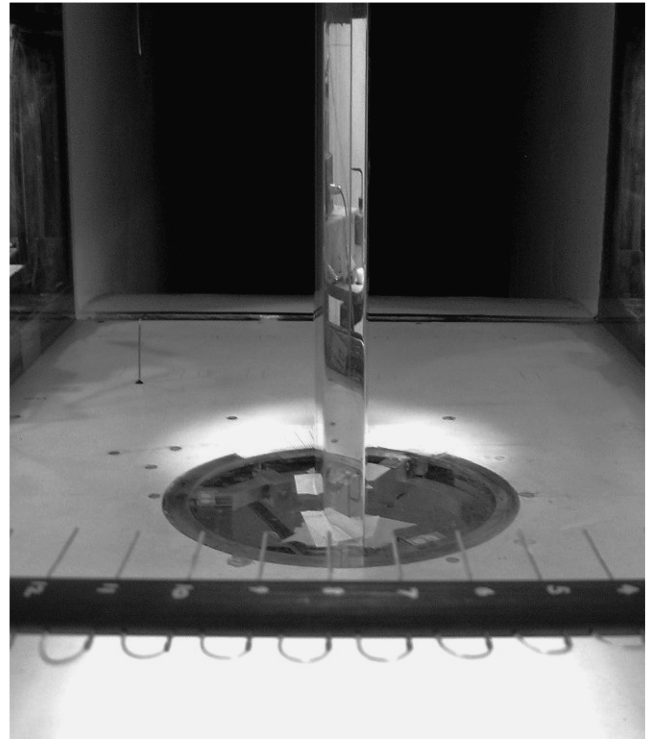


Fig. 3 Photograph of the NACA0021 mounted in the wind tunnel with wake rake.

momentum deficit in its wake. Although the pitot tubes spanned most of the tunnel width, the rake was mounted on a traversing mechanism that had a total travel comparable with the spacing between adjacent tubes. In this manner, one could traverse the wake, acquiring the necessary data for the experiment. There were also static pressure tubes in the rake that enabled the measurements of the static pressure variations across the two sides of the wake of the airfoil and enabled correcting the drag results that depend on these static pressure variations.

## III. Actuator Calibration

The momentum input of the plasma actuators was measured with a hot wire with no imposed flow, as shown in Fig. 4. The hot wire was placed as close to the plasma actuator as possible. At the location shown in the photo, the airflow from the actuator was already equal to the ambient temperature in the room, and thus the results are moderately accurate. The actuators were operated at  $\pm 5$  kV with a carrier frequency of 5 kHz. The velocities were measured at 100% duty cycle (continuous) and with a pulse-width-modulated signal corresponding to an  $F^+$  of 1 and a 10% duty cycle. The calibration could have been done in the wind tunnel using an optical method (laser Doppler anemometry or particle image velocimetry), as it was done by Göksel et al. [8,9], but the results did not warrant the additional effort and complexity.

Göksel et al. [8,9] suggested that plasma actuators provide too low of a momentum to be applied to general aviation, but may only be applicable to micro air vehicles at Reynolds numbers on the order of

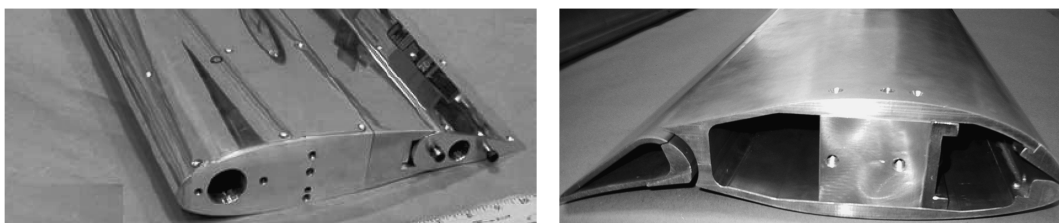


Fig. 2 Photographs of the NACA0021 (left) and the tiltrotor airfoil (right).

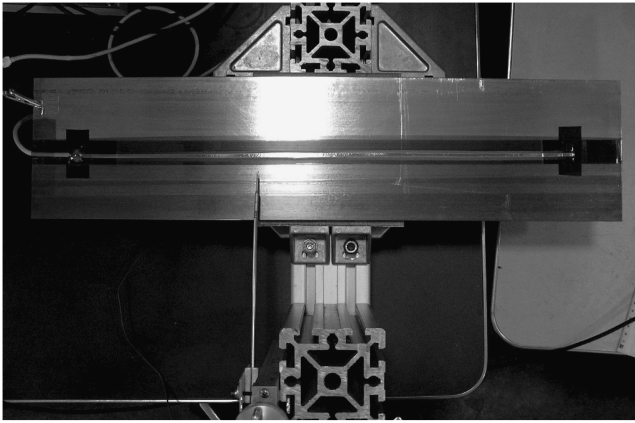


Fig. 4 Plasma calibration setup.

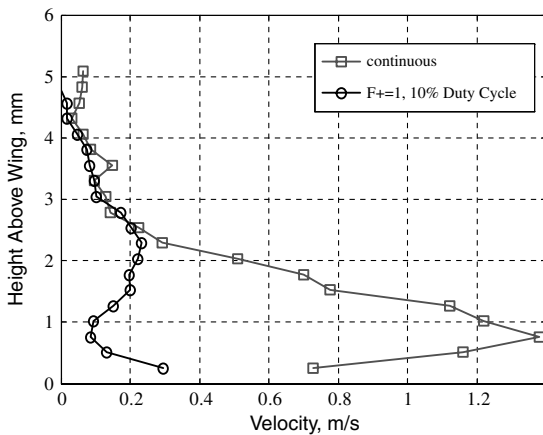


Fig. 5 Actuator calibration curves, velocity as function of height above airfoil surface.

10,000. The velocity profiles measured downstream of the plasma actuators used in this study are shown in Fig. 5 and confirm Göksel et al.'s assertions. When the plasma actuation was applied continuously, the integrated  $C_\mu$  for the NACA0021 airfoil with a  $U_\mu$  of 5 m/s (corresponding to a Reynolds number of 100,000) was less than 0.08%. With a 10% duty cycle that corresponds approximately to  $F^+ = 1$ , useful for flow separation control, the resulting  $C_\mu$  is, at most, one-fifth of this value, or less than 0.02%. At larger Reynolds number or at low burst rates, the input amplitude becomes insignificant. For example, at a Reynolds number of 200,000 and a duty cycle of 5% pulsed at  $F^+ = 1$ , the estimated  $C_\mu$  is approximately 0.001%.

#### IV. NACA0021 Test Results

The plasma actuators were located near the leading edge, where they could affect transition and leading-edge separation, and at the flap shoulder, where they had the largest possibility to influence reattachment of the flow over a deflected flap. The results obtained using plasma actuation were then compared with the effectiveness of roughness strips and, in one case, with vortex generators. For all tests, the actuators were operated at  $\pm 5$  kV with a carrier frequency of 5 KHz, a duty cycle of 10%, and  $F^+ = 1$ .

Experiments carried out on the clean baseline airfoil with no flap deflection ( $\delta_f = 0^\circ$ ) and no actuators at the two Reynolds numbers considered (100,000 and 200,000) indicate that the maximum slope of the lift curve ( $dC_L/d\alpha$ ) is approximately  $2\pi(1 + t/c)$ , or 0.132/deg. This slope is higher than commonly used in conjunction with thin airfoil theory, because the airfoil is 21% thick. The maximum lift slope is only sustainable over a narrow range of angles between 6 and 8 deg for a Reynolds number of 200,000 and between 2 and 6 deg for a Reynolds number of 100,000. There is a

break in the  $dC_L/d\alpha$  slope that is most obvious when the airfoil is clean, as shown in Figs. 6 and 7. It is associated with the large bubble that is generated on the upper loft of the airfoil that becomes smaller as  $\alpha$  increases. The decrease in the extent of the bubble stems from the adverse pressure gradient that becomes more severe with increasing incidence, and with it, there is a decrease in the lift increment. The creation of the large bubble at small values of  $C_L$  may also be the reason for the large values of  $dC_L/d\alpha$  at small angles of incidence.

The deflection of the trailing-edge flap increases the circulation around the airfoil, resulting in an earlier generation (at smaller values of  $\alpha$ ) of the large bubble; this increases the maximum  $dC_L/d\alpha$  to 0.26 for a  $\alpha$  between  $-4$  and  $0^\circ$  (Fig. 7). As the bubble gets squeezed out between  $0$  and  $12^\circ$ , the lift slope decreases to approximately 0.04 for  $\delta_f = 15^\circ$ . Consequently, the initially large value of  $dC_L/d\alpha$  that approximates inviscid airfoil theory has been generated by a mechanism that has little in common with inviscid flow or a high Reynolds number flow possessing a thin boundary layer. It is an outcome of a shear layer instability that generates large eddies responsible for the reattachment of the flow to the surface. This instability is affected by the pressure gradient that shortens the bubble and reduces the lift increment.

Simply installing the PA near the leading edge, but not activating it (referred to as PA baseline in Fig. 7), slightly reduced the initial  $dC_L/d\alpha$  slope as well as the lift at which the break in  $dC_L/d\alpha$  occurred. Consequently, the maximum lift attained by the airfoil ( $C_{L,max}$ ) was also reduced, although the stall angle  $\alpha_{stall}$  was increased by  $2^\circ$  to  $4^\circ$ . The penalty associated with having the static actuator near the leading edge may be as high as a 0.2 decrease in  $C_{L,max}$  (Figs. 6 and 7). The inactive plasma actuator provided a surface discontinuity and a disturbance that shortened the bubble and thus reduced the lift. This effect could be eliminated with an actuator design that conforms more closely to the clean-wing profile. Activating the plasma by a burst mode at  $F^+ = 1$  increased the disturbance level, thus further reducing the initial  $dC_L/d\alpha$  and increasing  $\alpha_{stall}$ . The additional lift generated by the increase in  $\alpha_{stall}$  helped to recover some of the lift lost at smaller values of  $\alpha$ . Thus, the  $C_{L,max}$  was approximately equal to the  $C_{L,max}$  attained with the passive actuator when the flap was not deflected and with the  $C_{L,max}$  obtained by the clean airfoil when  $\delta_f = 15^\circ$ .

The addition of the passive actuator at an  $x/c$  of 0.05 reduced the drag of the clean airfoil by approximately 20% over most of the useful range of incidence angles at  $Re = 100,000$ , but it had no substantial effect at  $Re = 200,000$ . The disturbance that it generated reduced the size of the bubble, but it apparently did not contribute to the loss of momentum downstream of the bubble reattachment location. Plasma actuation eliminated the bubble over most of the airfoil's upper loft, but the eddies that it generated at  $F^+ = 1$  increased the skin friction. Consequently, in the operational  $C_L$  range of 0.6 to 0.8, the presence of the passive actuator renders a superior performance. Placing the passive actuator at  $x/c = 0.65$ , near the leading edge of the flap, did not affect the bubble that was located upstream of it, but it caused an earlier separation over the flap and hence an increase in drag. Thus, around a  $C_L$  0.5 to 0.8, the location of the passive actuator may affect the drag by as much as 30%. The plasma actuation at this location, although the flap was not deflected, provided no benefit whatsoever, but it was not deleterious as it was when being located at  $x/c = 0.05$ .

Replacement of the plasma actuator by a roughness strip (made of an array of Vs embossed on an adhesive label) increased the  $C_{L,max}$  by 14%. This is shown in Fig. 8. This result was superior to the performance of the plasma actuators and it led to the consideration of replacing the plasma actuators by a simple row of vortex generators, also shown in Fig. 8. The improvement in the maximum lift generated by the vortex generators was not substantial, but the stall characteristics of the airfoil were vastly improved. The introduction of vortex generators had an adverse effect on the drag of the airfoil when compared with the embossed-V roughness strip or with the passive actuator.

The pressure distribution over the airfoil at an  $\alpha$  of  $8^\circ$  and a  $\delta_f$  of  $0^\circ$  is shown in Fig. 9. At this  $\alpha$ , the flow is attached over the aft portion of the airfoil, but a bubble is present on its upper loft.

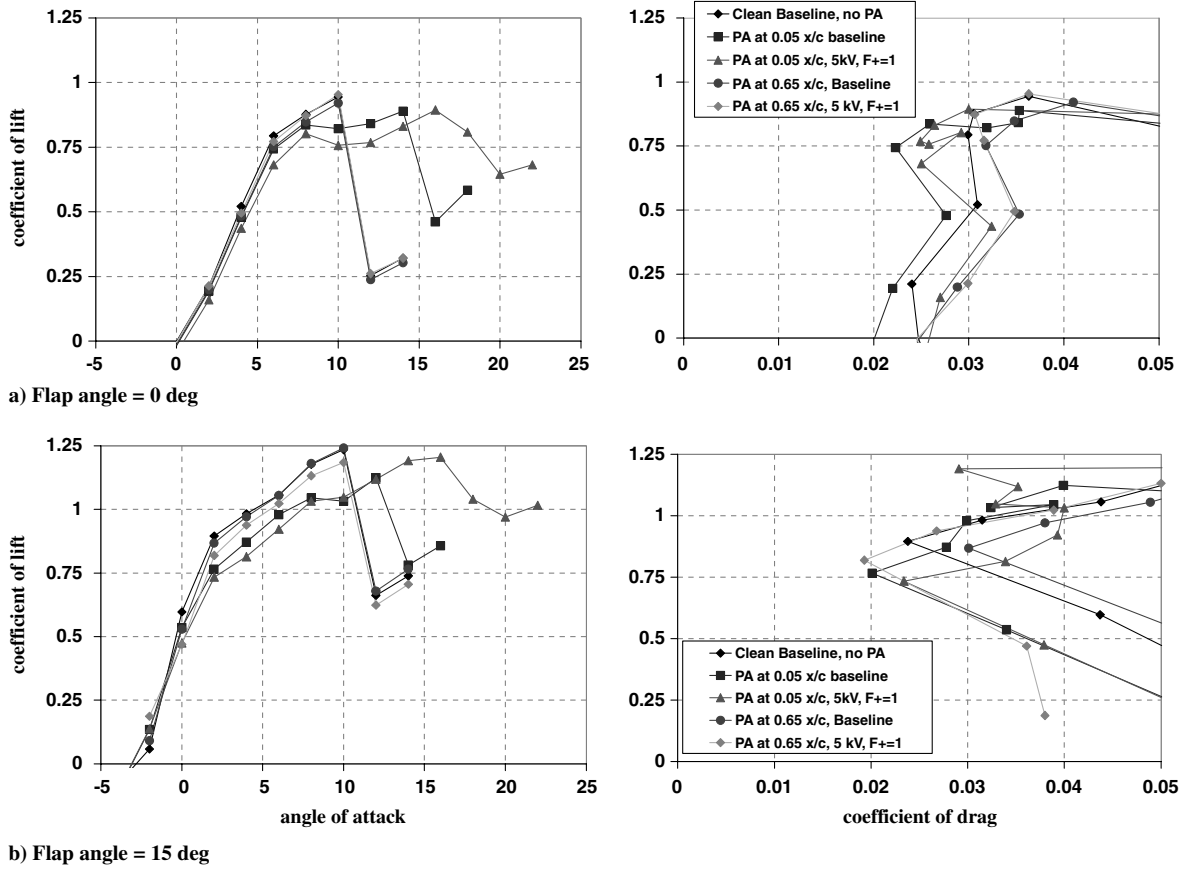


Fig. 6 Dependence of  $C_L$  on  $\alpha$  and the corresponding drag polar at  $Re = 100,000$ : a)  $\delta_f = 0$  deg and b)  $\delta_f = 15$  deg; with no actuators installed (clean) and with and without active actuators, as specified in the figure.

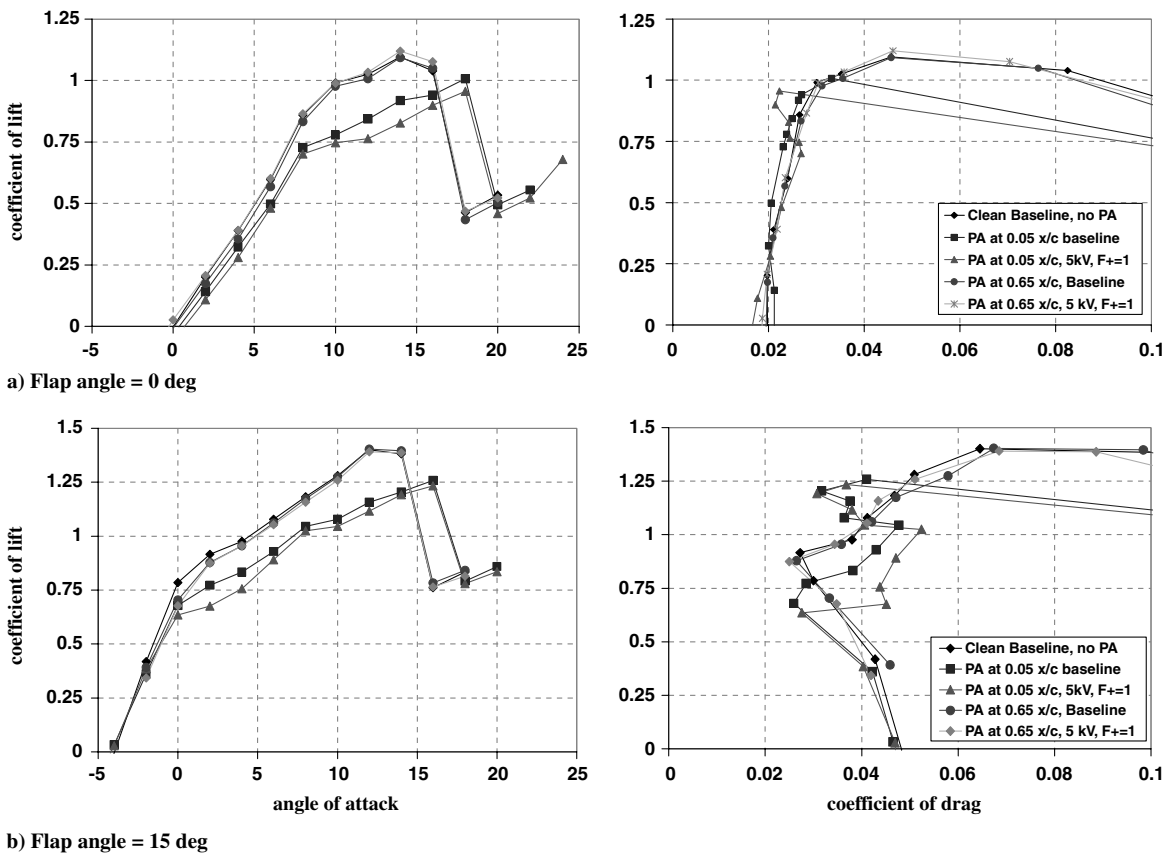


Fig. 7 Dependence of  $C_L$  on  $\alpha$  and the corresponding drag polar at  $Re = 200,000$ : a)  $\delta_f = 0$  deg and b)  $\delta_f = 15$  deg; with no actuators installed (clean) and with and without active actuators, as specified in the figure.

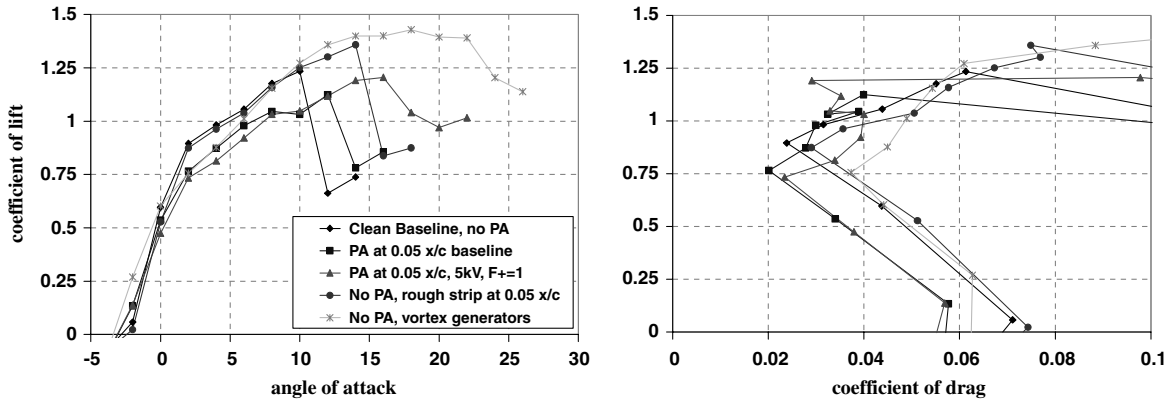


Fig. 8 Comparing the performance of the airfoil due to plasma actuation and a roughness strip or vortex generators replacing the actuators at the same location:  $Re = 100,000$ .

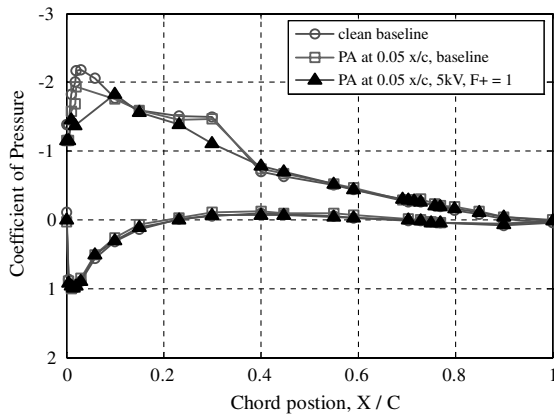


Fig. 9 Comparison of  $C_p$  distributions for  $\alpha = 8$  deg,  $\delta_f = 0$  deg, and  $Re = 100,000$  on the NACA0021: no PA, PA inactive, and PA active.

The bubble terminates around  $x/c = 0.3$  with and without the passive actuator being present. The presence of the passive actuator spoils the flow near the leading edge, reducing the minimum pressure there. When the plasma actuator is turned on, the bubble is entirely eliminated, but the minimum pressure near the leading edge is also lowered, thus whereas  $C_{p\min}$  was  $-2.2$  for the clean airfoil, it was only  $-1.9$  with passive actuator and even less when the plasma was active.

Increasing the incidence from 4 to 14 deg with the passive actuators present continually reduced the size of the bubble, as shown in Fig. 10. This is caused by the enhanced adverse pressure gradient that destabilizes the flow, resulting in an earlier transition to turbulence. Instability and transition result in an earlier closure of the

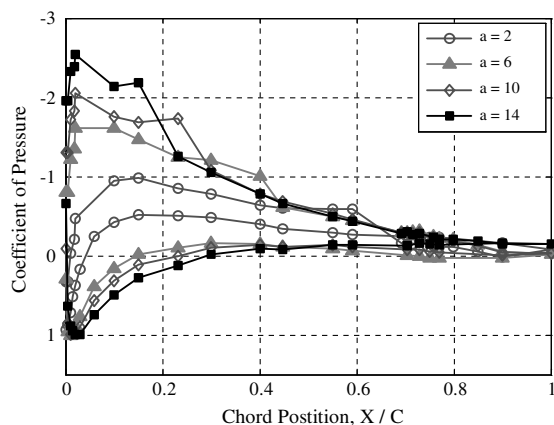


Fig. 10 Comparison of  $C_p$  distributions for  $\alpha = 2$ –14 deg,  $\delta_f = 0$  deg, and  $Re = 100,000$  with passive actuator installed at 5% chord.

bubble. Thus, whereas at an  $\alpha$  of 4 deg the leading-edge bubble terminates around  $x/c \approx 0.5$ , at an  $\alpha$  of 14 deg, it does so at  $x/c \approx 0.15$ .

Although activating the plasma actuation at  $x/c = 0.05$  eliminated the bubble, it also lowered the level of the minimum pressure near the leading edge, as shown in Fig. 11. For example, with a passive actuator,  $C_{p\min}$  was  $-2.5$  at an  $\alpha$  of 14 deg and it dropped to  $-2$  with an active plasma actuator. Thus, plasma actuation promoted transition to turbulence and somewhat reduced the lift attained at a given incidence.

Pressure distributions over a range of incident angles with an active plasma actuator placed at the flap shoulder (i.e.,  $x/c = 0.65$ ) are shown in Fig. 12. The actuator had no effect on the bubble upstream. This is also an indicator that the momentum coefficient of actuation is so small that it does not generate any suction (sink effect) upstream of it. Periodic excitation generates such suction at low  $C_\mu$ , even if it fails to reattach the flow downstream. Also note that the airfoil stalled at a lower incidence than it did in the presence of a roughness strip or an actuator at the leading edge.

Replacing the actuators with vortex generators maintained the flow attached to a flap deflected to 15 deg ( $\delta_f = 15$  deg) up to an  $\alpha$  of 14 deg, as shown in Fig. 13. At an  $\alpha$  of 16 deg, the flow separated over 50% of the chord (i.e., the flow over the deflected flap was fully separated), but this did not prevent the generation of high lift up to an  $\alpha$  of 22 deg, because the flow in the leading-edge region remained attached, providing a  $C_{p\min}$  less than  $-4$ . At an  $\alpha$  of 24 deg, the flow finally separated near the leading edge, resulting in a decrease of lift. Thus, vortex generators are much more effective in delaying separation than the plasma actuators, even at the low Reynolds number of 100,000. Doubling the Reynolds number tripped the boundary layer and eliminated all the benefits that the plasma actuators provided at a Reynolds number of 100,000.

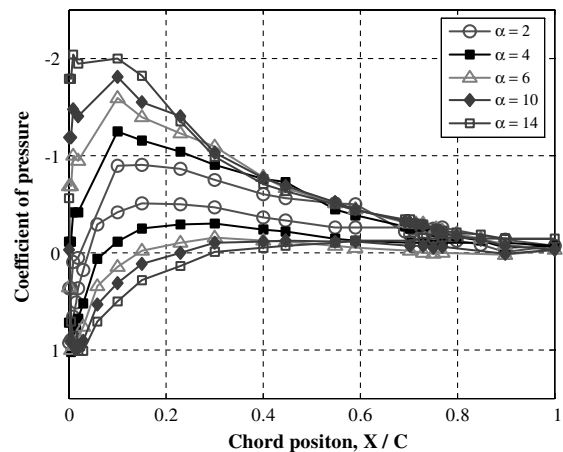


Fig. 11 Comparison of  $C_p$  distributions for  $\alpha = 2$ –14 deg,  $\delta_f = 0$  deg, and  $Re = 100,000$  with active plasma actuator at 5% chord.

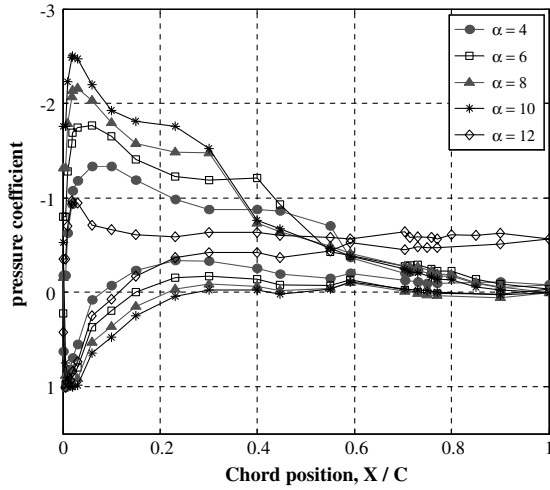


Fig. 12 Comparison of  $C_p$  distributions for  $\alpha = 4$ – $12$  deg,  $\delta_f = 0$  deg, and  $Re = 100,000$  with active plasma actuator at 65% chord.

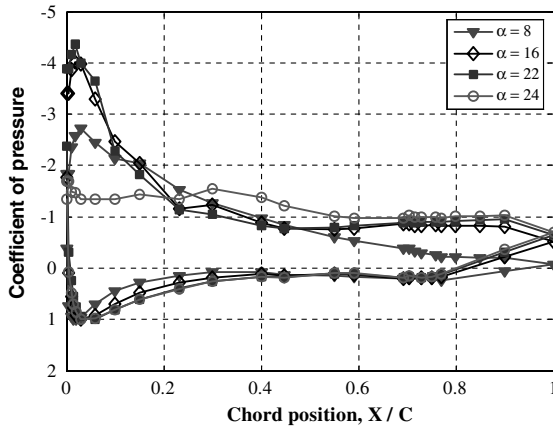


Fig. 13 Comparison of  $C_p$  distribution for  $\alpha = 0$ – $24$  deg,  $\delta_f = 15$  deg when vortex generators were used at  $Re = 100,000$ .

## V. Tiltrotor Airfoil Tests Results

The role of the plasma actuators as transition accelerators is demonstrated again on the tiltrotor airfoil by comparing the data obtained at two Reynolds numbers: 83,000 and 250,000. This airfoil was chosen not only because of its availability and utility, but also because it has a relatively flat pressure distribution over its upper loft. At a Reynolds number of 250,000, this feature is not as susceptible to the creation of a large bubble over its upper surface as was the case with the NACA0021. At much lower Reynolds numbers, it is also susceptible to laminar flow separation in spite of the roughness strips that were normally used when the airfoil was tested at intermediate Reynolds numbers. For all tests, the actuators were operated at  $\pm 5$  kV with a carrier frequency of 5 KHz, a duty cycle of 10%, and  $F^+ = 1$ .

Data taken at a Reynolds number of 83,000 and a  $\delta_f$  of 0 deg are shown in Fig. 14. The roughness strips were indeed insufficient to trigger transition to turbulence, and thus in the absence of the actuator, the flow over the upper surface of the airfoil was separated. This resulted in a  $dC_L/d\alpha$  slope of 0.05/deg. The mere presence of the plasma actuators provided an additional two-dimensional protuberance that tripped the boundary layer at higher angles of incidence; consequently, at an  $\alpha$  of 6 deg, the lift increased from a  $C_L$  of 0.25 to a  $C_L$  of 1. Activating the plasma actuator located near the leading edge provided an effective trip that delayed the stall angle to an  $\alpha$  of 14 deg and increased  $C_{L,max}$  to 1.45. Activating the plasma actuator at the flap shoulder (i.e., at  $x/c = 0.75$ ) was not as effective (a  $C_{L,max}$  of 1.27 at an  $\alpha$  of 8 deg), because the upstream boundary layer was not turbulent and a large bubble was generated.

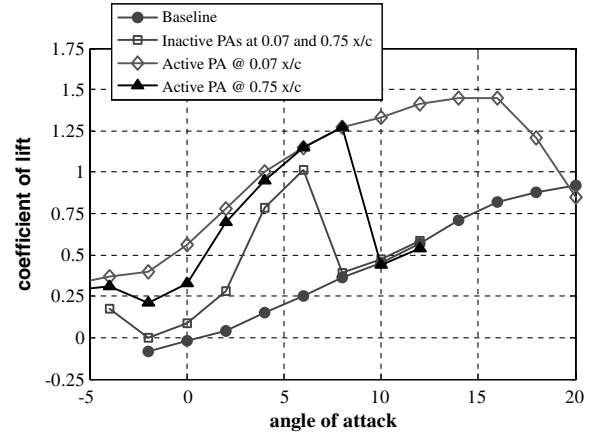


Fig. 14 Dependence of  $C_L$  on  $\alpha$  at  $\delta_f = 0$  deg and  $Re = 83,000$  without plasma actuators installed (clean) and with and without active actuators as specified in the figure.

Similar data taken at a Reynolds number of 250,000 and a  $\delta_f$  of 0 deg are shown in Fig. 15. The reverse observation of that seen at a Reynolds number of 83,000 can be made. The roughness strips are effective, and under these circumstances, the plasma actuation is not beneficial. In the absence of the actuators, the  $C_{L,max}$  is 1.87, whereas in their inactive presence,  $\alpha_{stall}$  increased to 20 deg but  $C_{L,max}$  dropped to 1.72. Activating the plasma actuator located near the leading edge also results in local decrease of lift at an  $\alpha$  of 8 deg that is followed up by a relative increase in the  $dC_L/d\alpha$  when  $\alpha$  is less than 16 deg, but it reduced  $C_{L,max}$  to 1.65.

With the flap deflected at a  $\delta_f$  of 15 deg in the absence of actuators, at the lower Reynolds number, there is a substantial increase in the lift, as shown in Fig. 16. This is because the deflected flap increased the circulation around the airfoil, altering the pressure gradient that led to earlier transition to turbulence. Consequently, in the absence of the plasma actuators, the maximum lift attained was a  $C_{L,max}$  of 1.6 at an  $\alpha$  of 6 deg. With the actuators present but inactive, the lift was higher at small angles of incidence, but it attained a  $C_{L,max}$  of only 1.5, also at an  $\alpha$  of 6 deg. It implies that the added two-dimensional protuberance that enabled transition at lower incidence simply added to the drag in a region in which transition occurred naturally. Activating the plasma actuator located near the leading edge boosted  $C_{L,max}$  to 1.9 at an  $\alpha$  of 12 deg, whereas activating the actuator located at the flap shoulder attained the same  $C_{L,max}$  at an  $\alpha$  of 4 deg. Consequently, the actuation at the flap shoulder is much more effective in maintaining the flow attached over the flap than the leading-edge actuation. In this case, a genuine separation control might have been achieved with  $C_\mu$  of less than 0.1%.

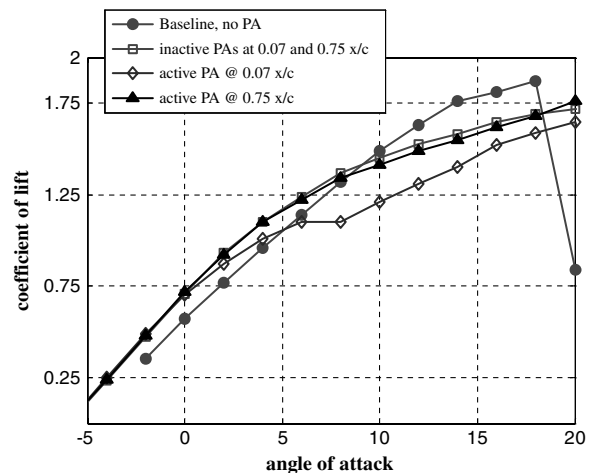


Fig. 15 Dependence of  $C_L$  on  $\alpha$  at  $\delta_f = 0$  deg and  $Re = 250,000$  without plasma actuators installed (clean) and with and without active actuators as specified in the figure.

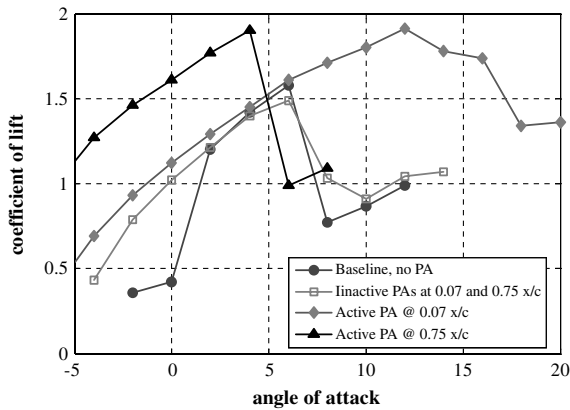


Fig. 16 Dependence of  $C_L$  on  $\alpha$  at  $\delta_f = 15$  deg and  $Re = 83,000$ , without plasma actuators installed (clean) and with and without active actuators as specified in the figure.

At a Reynolds number of 250,000 with the flap deflected at a  $\delta_f$  of 15 deg in the absence of actuators, the roughness strips were sufficient to trip the boundary layer and delay the occurrence of stall to a  $\alpha_{\text{stall}}$  of 14 deg and yielded a  $C_{L\text{max}}$  of 2.36, as shown in Fig. 17. The passive actuators presence increased  $\alpha_{\text{stall}}$  to 18 deg but concomitantly decreased  $C_{L\text{max}}$  to 2.06. Activating the actuator near the leading edge is deleterious, as it accelerated the separation from the flap, causing a kink in the  $dC_L/d\alpha$  slope around an  $\alpha$  of 10 deg and reducing the  $C_{L\text{max}}$  to 1.97. On the other hand, activating the actuator near the flap shoulder proved to be effective, increasing the

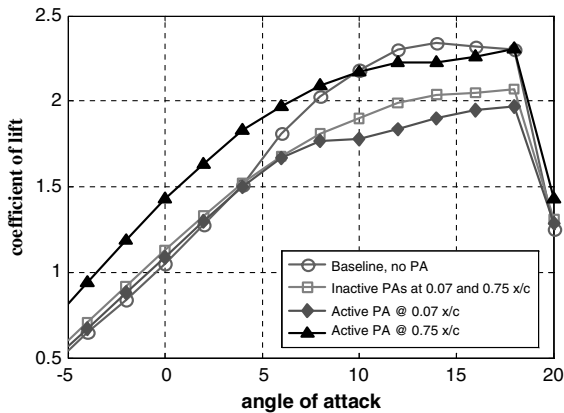
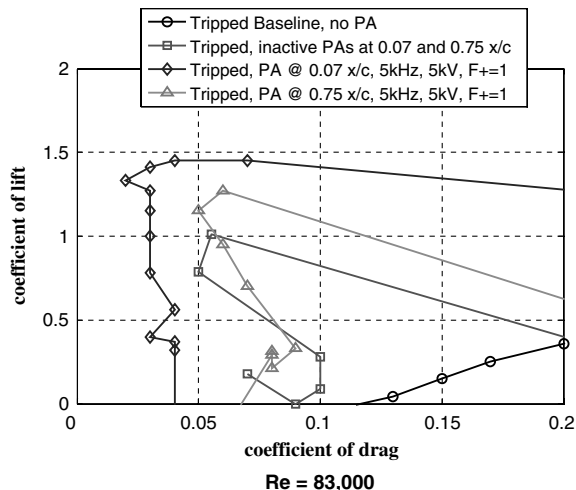


Fig. 17 Dependence of  $C_L$  on  $\alpha$  at  $\delta_f = 15$  deg and  $Re = 250,000$ , without plasma actuators installed (clean) and with and without active actuators as specified in the figure.



$dC_L/d\alpha$  slope throughout the useful range of  $\alpha$  less than 8 deg and increasing  $C_{L\text{max}}$  to almost that achieved in the absence of actuators (i.e.,  $C_{L\text{max}} = 2.30$ ).

The drag polars for a Reynolds number of 83,000 and 250,000 and a  $\delta_f$  of 0 deg are shown in Fig. 18. At a Reynolds number of 83,000, the drag polars indicate that actuation from the leading-edge region reduces the drag, regardless of the flap deflection angle, but it is completely ineffective at a Reynolds number of 250,000. It is known that even a very small addition of momentum may reduce drag if it results in the slightest attachment of the flow; this might be the case at the low Reynolds number range. On the other hand, actuators located at the flap shoulder increase the drag at all useful angles of incidence regardless of the flap deflection angle and Reynolds number.

The pressure distributions taken at an incidence of 4 deg and a  $\delta_f$  of 0 deg are shown in Fig. 19 and explain the effects of the plasma actuators on the performance of the airfoil at a Reynolds number of 83,000 and a  $\delta_f$  of 0 deg. The roughness strips used did not trigger transition, and the laminar boundary layer separated at an  $x/c$  of around 0.2. The addition of the passive actuators provides a 2-D protuberance that accelerates transition and creates a bubble that terminates at approximately  $x/c = 0.5$ . Because turbulent flow is attached over the airfoil at this incidence, substantial lift has been generated. Actuation over the flap shoulder lowers the pressure upstream but does not affect the trailing edge of the bubble, as it does not contribute to tripping, whereas periodic actuation at the leading edge affects transition, reducing the bubble size and thus increasing the lift. The readings of pressure near the leading edge on the upper loft are probably incorrect, due to the presence of the actuator.

Increasing the flap deflection to 15 deg increases the circulation over the airfoil and moves the stagnation point on the lower loft

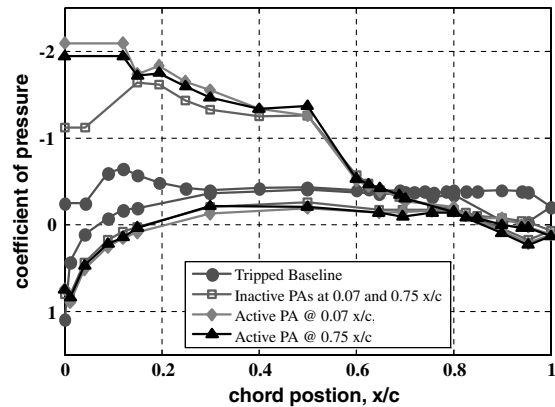


Fig. 19 Comparison of  $C_p$  distribution for  $\alpha = 4$  deg and  $\delta_f = 0$  deg at  $Re = 83,000$ ; without plasma actuators installed (clean) and with and without active actuators as specified in the figure.

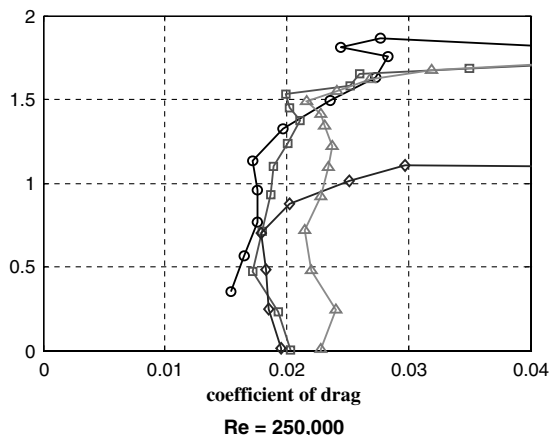


Fig. 18 Drag polars corresponding to  $\delta_f = 0$  deg at  $Re = 83,000$  and 250,000.

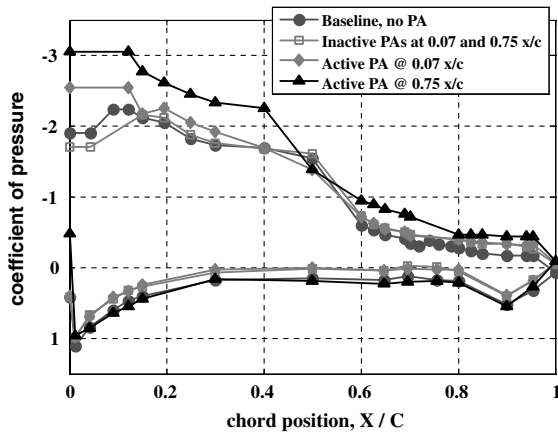


Fig. 20 Comparison of  $C_p$  distribution for  $\alpha = 4$  deg and  $\delta_f = 15$  deg at  $Re = 83,000$  without plasma actuators installed (clean) and with and without active actuators as specified in the figure.

toward the rear, as shown in Fig. 20. This in turn triggers transition, even in the absence of the actuators, and generates lift. The addition of the passive actuator near the leading edge depletes some of the momentum from the boundary layer and results in an earlier separation over the flap, thus lowering the lift somewhat. A bubble is still present in both cases at  $x/c = 0.5$ . Plasma actuation from the leading-edge region did not have any effect on the pressure distribution over the flap, but simply eliminated the bubble located at its wake, lowering the pressure in the leading-edge region. Actuation over the flap shoulder attached the flow over the leading portion of the flap and shortened the bubble upstream, thus genuinely substantially increasing the circulation over the airfoil.

## VI. Improved Actuators and System Integration

There are many improved plasma actuator technologies currently under development; however, many of these significantly increase the complexity of the actuation system, negating the primary benefits of SDBP: namely, their robustness, simple construction, and low weight.

There have been very few published assessments of the practical issues associated with integrating effective SDBD actuators into a realistic aircraft system operating at high Reynolds numbers and high speeds. For example, recent studies have shown that the momentum output decreases significantly at low ambient pressures, making their applicability to high-altitude applications questionable [10,11].

New high-voltage plasma actuators have been developed that provide considerably greater authority and correspondingly greater potential as active flow control actuators. Figure 21 compares the performance of the actuators used in the wind-tunnel testing reported in this paper with recent laboratory tests of high-voltage plasma actuators. The output thrust has increase by a factor of 20 by

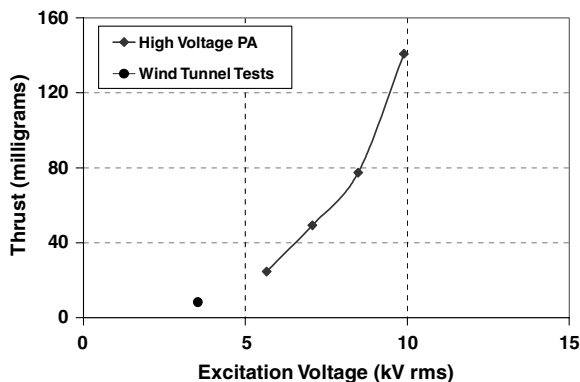


Fig. 21 Improved high-voltage plasma actuators compared with actuators used in this study.

employing thicker dielectric (up to 1 mm thick) at greatly increased voltages of 3.5 to 10 kV rms. Although this provides hope for improved performance of plasma actuators for active flow control, there are considerable issues that need to be addressed. The supporting technologies such as lightweight amplifiers that are capable of such high voltages require maturation.

Several test studies and models have shown that the plasma actuator performance can be improved by driving them with biased nanosecond pulses [12,13]. Although early indications are good, the pulses are difficult to create and raise the issue of electromagnetic radiation and interference. These issues will need to be solved before they can be practically implemented. Roupassov et al. [14] concluded that the mechanism for the plasma actuator operating with nanosecond pulses is different from the boundary momentum transfer seen in the ac-driven actuators, indicating that much work needs to be done before it is truly understood.

## VII. Conclusions

Current practical SDBD plasma actuators do not provide sufficient momentum to prevent separation at  $Re > 100,000$ , unless the velocity at the higher Reynolds numbers is very low. Under special circumstances, their passive presence on the surface may trip the boundary layer, making it more resistant to separation; however, in those cases, a proper roughness strip or vortex generators may delay separation more effectively. Because the periodic component of the actuation when plasma is used is relatively small, plasma actuators may have a deleterious effect on the flow, and rather than suppressing separation, they actually promote it. At very low Reynolds numbers that are appropriate to micro air vehicles, plasma actuators may provide sufficient momentum to be effective in delaying separation.

New plasma actuator technologies may provide considerably greater authority and correspondingly greater potential as active flow control actuators; however, the supporting technologies such as complex power amplifiers and materials that are capable of such high voltages and temperatures require maturation. And considerable work needs to be done to integrate such actuators into aerospace structures.

## References

- [1] Enloe, C., McLaughlin, T., VanDyken, D., Kachner, K., Jumper, E., and Corke, T., "Mechanisms and Response of a Single Dielectric Barrier Plasma Actuator: Plasma Morphology," *AIAA Journal*, Vol. 42, No. 3, pp. 589–594. doi:10.2514/1.2305; also AIAA Paper 2003-1021.
- [2] Enloe, C., McLaughlin, T., VanDyken, D., Kachner, K., Jumper, E., Corke, T., Post, M., and Haddad, O., "Mechanisms and Response of a Single Dielectric Barrier Plasma Actuator: Geometric Effects," *AIAA Journal*, Vol. 42, No. 3, 2004, pp. 595–604. doi:10.2514/1.3884
- [3] Post, M., and Corke, T., "Separation Control on High Angle of Attack Airfoil Using Plasma Actuators," *AIAA Journal*, Vol. 42, No. 11, 2004, pp. 2177–2184. doi:10.2514/1.2929
- [4] Patel, M., Ng, T., Vasudevan, S., Corke, T., Post, M., McLaughlin, T., and Suchomel, C., "Scaling Effects of an Aerodynamic Plasma Actuator," *Journal of Aircraft*, Vol. 45, No. 1, 2008, pp. 223–236. doi:10.2514/1.31830
- [5] Porter, C., McLaughlin, T., Enloe, C., Font, G., Roney, J., and Baughn, J. W., "Boundary Layer Control Using a DBD Plasma Actuator," 45th AIAA Aerospace Sciences Meeting and Exhibit, Reno, NV, AIAA Paper 2007-786, Jan. 2007.
- [6] Huang, J., Corke, T., and Thomas, F., "Plasma Actuators for Separation Control of Low-Pressure Turbine Blades," *AIAA Journal*, Vol. 44, No. 1, 2006, pp. 51–57. doi:10.2514/1.2903
- [7] Corke, T., Post, M., and Orlov, D. M., "Single-Dielectric Barrier Discharge Plasma Enhanced Aerodynamics: Concepts, Optimization, and Applications," *Journal of Propulsion and Power*, Vol. 24, No. 5, Sept.–Oct. 2008, pp. 935–945. doi:10.2514/1.24430
- [8] Göksel, B., Greenblatt, D., Rechenberg, I., Singh, Y., Nayeri, C., and Paschereit, C., "Pulsed Plasma Actuators for Separation Flow Control," *Conference on Turbulence and Interactions (TI2006)*, Porquerolles,



- France, 29 May –2 June 2006, available online at [www.onera.fr/congres/ti2006/definitivepapers/Goeksel.pdf](http://www.onera.fr/congres/ti2006/definitivepapers/Goeksel.pdf).
- [9] Göksel, B., Greenblatt, D., Rechenberg, I., Nayeri, C., and Paschereit, C., “Steady and Unsteady Plasma Wall Jets for Separation and Circulation Control,” 3rd AIAA Flow Control Conference, San Francisco, AIAA Paper 2006-3686, June 2006.
  - [10] Abe, T., Takizawa, Y., Sato, S., and Kimura, N., “Experimental Study for Momentum Transfer in a Dielectric Barrier Discharge Plasma Actuator,” *AIAA Journal*, Vol. 46, No. 9, Sept. 2008, pp. 2248–2256. doi:10.2514/1.30985
  - [11] Gregory, J., Enloe, C., Font, G., and McLaughlin, T., “Force Production Mechanisms of a Dielectric-Barrier Discharge Plasma Actuator,” 45th AIAA Aerospace Sciences Meeting and Exhibit, Reno, NV, AIAA Paper 2007-185, Jan. 2007.
  - [12] Likhanskii, A., Shneider, M., Macheret, S., and Miles, R., “Modeling of Dielectric Barrier Discharge Plasma Actuators Driven by Repetitive Nanosecond Pulses,” *Physics of Plasmas*, Vol. 14, No. 7, 2007, Paper 073501. doi:10.1063/1.2744227
  - [13] Likhanskii, A., Shneider, M., Macheret, S., and Miles, R., “Optimization of Dielectric Barrier Discharge Plasma Actuators Driven by Repetitive Nanosecond Pulses,” 45th AIAA Aerospace Sciences Meeting and Exhibit, Reno, NV, AIAA Paper 2007-633, Jan. 2007.
  - [14] Roupasov, D., Nikipelov, A., Nudnova, M., and Starikovskii, A., “Flow Separation Control by Plasma Actuator with Nanosecond Pulse Periodic Discharge,” 46th AIAA Aerospace Sciences Meeting and Exhibit, Reno, NV, AIAA Paper 2008-1367, Jan. 2008.